Inorganic Chemistry

Article

Efficiency of the Refocused ^{31}P–^{29}Si MAS-*J*-INEPT NMR Experiment for the Characterization of Silicophosphate Crystalline Phases and Amorphous Gels

C. Coelho, T. Azaïs, L. Bonhomme-Coury, G. Laurent, and C. Bonhomme*

Université Pierre et Marie Curie-Paris 6, UMR 7574, Laboratoire Chimie de la Matière Condensée de Paris, Paris, F-75005 France

One- and two-dimensional refocused MAS-*J*-INEPT NMR experiments in the solid state (through-bond polarization transfer) involving the highly abundant ^{31}P spin and the rare ^{29}Si spin are described for the crystalline silicophosphate phase $Si_5O(PO_4)_6$ and complex mixtures of SiP_2O_7 polymorphs. The evaluation of the $^2J_{P-O-Si}$ coupling constants for all ^{29}Si sites is obtained by the careful analysis of the INEPT build-up curves under fast MAS. The results are in agreement with the crystallographic data, taking into account the various *J* coupling paths. The efficiency of the experiment is demonstrated by its application to more complex systems such as silicophosphate amorphous gels (obtained by the sol–gel process).

Introduction

Recently, silicophosphate gels and derivatives have gained much attention in various fields. Among them, we can cite (i) the study of gel-derived silicophosphate xerogels and glasses,[1–3] exhibiting interesting technological properties with application as fast proton conductors,[4] (ii) the study of surface grafting reactions between silica gels or nanoparticles and phosphate or phosphonate moieties,[5–6] (iii) the study of gels, precursors for the synthesis of microporous silicoalumino-phosphates (SAPO),[7–8] and *(iv)* the study of surfaces in biomaterials, involving bioactive phosphosilicates and sub-stituted hydroxyapatite (HAP) structures.[9] This vivid field of research includes the detailed study of silicon-substituted HAP, in terms of bone interfaces and bioactivity.[10] The surface modification of HAP by silica or silicates has been deeply investigated.[11] The formation of calcium phosphate in silica gels and the mechanisms of the bonelike formation of bioactive implants have also been reviewed.[12–14]

In the field of materials, the local structure of nuclei can be probed efficiently by solid-state NMR spectroscopy. In the case of silicophosphates, it is well-established that the

---

* To whom correspondence should be addressed. Phone: +33 1 44 27 41 35. Fax: +33 1 44 27 47 69. E-mail: bonhomme@ccr.jussieu.fr.

(1) (a) Clayden, N. J.; Esposito, S.; Pernice, P.; Aronne, A. *J. Mater. Chem.* **2001**, *11*, 936–943. (b) Livage, J.; Barboux, P.; Vandenborre, M. T.; Schmutz, C.; Taulelle, F. *J. Non-Cryst. Solids* **1992**, *147–148*, 18–23. (c) Tian, F.; Pan, L.; Wu, X. *J. Non-Cryst. Solids* **1988**, *104*, 129–134. (d) Szu, S. P.; Klein, L. C.; Greenblatt, M. *J. Non-Cryst. Solids* **1992**, *143*, 21–30. (e) Aronne, A.; Turco, M.; Bagnasco, G.; Pernice, P.; Di Serio, M.; Clayden, N. J.; Marenna, E. *Chem. Mater.* **2005**, *17*, 2081–2090.

(2) Coelho, C.; Azaïs, T.; Bonhomme-Coury, L.; Maquet, J.; Bonhomme, C. *C. R. Chim.* **2006**, *9*, 472–477.

(3) Coelho, C.; Babonneau, F.; Azaïs, T.; Bonhomme-Coury, L.; Maquet, J.; Laurent, G.; Bonhomme, C. *J. Sol-Gel Sci. Technol.* **2006**, *40*, 181–189.

(4) Nogami, M.; Miyamura, K.; Abe, Y. *J. Electrochem. Soc.* **1997**, *144*, 2175–2178.

(5) Lukes, I.; Borbaruah, M.; Quin, L. D. *J. Am. Chem. Soc.* **1994**, *116*, 1737–1741.

(6) Mutin, P. H.; Lafond, V.; Popa, A. F.; Granier, M.; Markey, L.; Dereux, A. *Chem. Mater.* **2004**, *16*, 5670–5675.

(7) Fyfe, C. A.; Wong-Moon, K. C.; Huang, Y.; Grondey, H. *Microporous Mater.* **1995**, *5*, 29–37.

(8) (a) Huang, Y.; Machado, D. *Microporous Mesoporous Mater.* **2001**, *47*, 195–202. (b) Huang, Y.; Machado, D.; Kirby, C. W. *J. Phys. Chem. B* **2004**, *108*, 1855–1865.

(9) (a) Hench, L. L. *J. Am. Ceram. Soc.* **1991**, *74*, 1487–1510. (b) Fujii, E.; Ohkubo, M.; Tsuru, K.; Hayakawa, S.; Osaka, A.; Kawabata, K.; Bonhomme, C. *Acta Biomater.* **2006**, *2*, 69–74. (c) Hayakawa, S.; Ohnishi, K.; Tsuru, K.; Osaka, A.; Fujii, E.; Kawabata, K.; Bonhomme, C.; Babonneau, F. *Key Eng. Mater.* **2006**, *309*, 503–506. (d) Hayakawa, S.; Ando, K.; Tsuru, K.; Osaka, A.; Fujii, E.; Kawabata, K.; Bonhomme, C.; Babonneau, F. *J. Am. Ceram. Soc.* **2007**, in press.

(10) (a) Porter, A. E.; Patel, N.; Skepper, J. N.; Best, S. M.; Bonfield, W. *Biomaterials* **2004**, *25*, 3303–3314. (b) Porter, A. E.; Patel, N.; Skepper, J. N.; Best, S. M.; Bonfield, W. *Biomaterials* **2003**, *24*, 4609–4620.

(11) (a) Borum, L.; Wilson, O. C., Jr. *Biomaterials* **2003**, *24*, 3681–3688. (b) Liu, X.; Ding, C.; Chu, P. K. *Biomaterials* **2004**, *25*, 1755–1761.

(12) Korventausta, J.; Jokinen, M.; Rosling, A.; Peltola, T.; Yli-Urpo, A. *Biomaterials* **2003**, *24*, 5173–5182.

(13) De Aza, P. N.; Luklinska, Z. B.; Santos, C.; Guitian, F.; De Aza, S. *Biomaterials* **2003**, *24*, 1437–1445.

(14) Handke, M.; Sitarz, M.; Rokita, M.; Galuskin, E. *J. Mol. Struct.* **2003**, *651–653*, 39–54.

---

isotropic ^{31}P and ^{29}Si chemical shifts (δ_{iso}) can be assigned to the Q_N and Q'_N species, where Q_N is related to the $Si(OX)_N(OX')_{4-N}$ moieties (with X = Si, P; X' = H, Et) and Q'_N stands for $P(O)(OY)_N(OY')_{3-N}$ entities (with Y = P, Si ; Y' = H).[1d] Nevertheless, we have shown recently that these notations are rather loose, in the sense that various combinations of P−O−P/P−O−Si/P−OH··· bonds can lead to the same δ_{iso} value.[3] In other words, sole knowledge of the chemical shift values is not sufficient for the fine structural description of silicophosphate derivatives.

Various solid-state NMR techniques can be implemented for establishing the *connectivities* between nuclei (*i.e.,* ^{29}Si and ^{31}P). The experiments used so far can be divided roughly in two main categories.

The first category includes *D*-mediated experiments, where *D* stands for the heteronuclear or homonuclear dipolar interactions. Such experiments establish *spatial connectivities* between X and Y nuclei. In the case of the *heteronuclear* dipolar interaction (X ≠ Y), REDOR (rotational-echo double resonance),[15] TEDOR (transferred-echo double resonance), TRAPDOR (transfer of polarization in double resonance),[16] and CP MAS[17−18] (cross polarization magic angle spinning) pulse sequences are usually implemented. In some cases, the distances between nuclei were accurately measured by the careful analysis of the dipolar oscillations.[19−20] For X = ^{31}P and Y = ^{29}Si, very few results have been reported so far in the literature. These results are related to silicon phosphide (involving direct ^{31}P−^{29}Si bonds)[21] and silicophosphate phases involving ^{31}P−O−^{29}Si groups.[2,22] Triple resonance experiments $^{1}H \rightarrow {}^{31}P \rightarrow {}^{29}Si$ were used for editing purposes in silicophosphate gels.[2] The crystalline $Si_5O(PO_4)_6$ phase was used as a standard for the setup of the $^{31}P \rightarrow {}^{29}Si$ 2D HETCOR (heteronuclear correlation) CP MAS experiment.[22] It has to be noted that because of the small ^{31}P−^{29}Si dipolar couplings (∼360 Hz), very long contact times (up to 40 ms) were used under the Hartmann−Hahn condition. Such experimental conditions are very demanding in terms of probe coil and RF power levels. In the case of the *homonuclear* dipolar interaction (X = Y), recoupling tech-

niques,[23] as well as spin diffusion experiments,[23a,24] were successfully used in the frame of inorganic phosphates.

The second category includes *J*-mediated experiments, where *J* stands for the heteronuclear or homonuclear isotropic scalar coupling. In the early 1990's, such NMR sequences were implemented by Fyfe and co-workers[25] and Eckert and co-workers.[26] In the late 1990's, Emsley and co-workers showed that the INADEQUATE (incredible natural abundance double quantum transfer experiment)[27] and the HMQC (heteronuclear multiple quantum coherence)[28] sequences could be safely transposed in solid-state NMR for the study of organic and bio-organic derivatives. The *homonuclear* INADEQUATE and UC2QF COSY (uniform-sign cross-peak double quantum filtered correlation spectroscopy) sequences have been subsequently used for the following spin pairs: $^{31}P/^{31}P$, $^{29}Si/^{29}Si$, $^{15}N/^{15}N$, and $^{13}C/^{13}C$.[23c−e,29−32] The *heteronuclear* HMQC sequence was adapted for the following spin pairs: $^{1}H/^{13}C$, $^{1}H/^{15}N$, $^{31}P/^{27}Al$, $^{27}Al/^{17}O$, $^{31}P/^{29}Si$, and $^{31}P/^{71}Ga$.[26,28,33−36] More involved *J*-derived solid-state NMR techniques were proposed recently in the literature, including triple quantum correlation experiments,[37] 2D and 3D H-HSQC (homonuclear-heteronuclear single quantum correlation) experiments,[38] and frequency-selective

(15) Gullion, T.; Schaefer, J. *J. Magn. Reson.* **1989**, *81*, 196−200.
(16) (a) Hing, A. W.; Vega, S.; Schaefer, J. *J. Magn. Reson.* **1992**, *96*, 205−209. (b) Grey, C. P.; Vega, A. J. *J. Am. Chem. Soc.* **1995**, *117*, 8232−8242.
(17) Hartmann, S. R.; Hahn, E. L. *Phys. Rev.* **1962**, *128*, 2042−2053.
(18) Pines, A.; Gibby, G.; Waugh, J. S. *J. Chem. Phys.* **1973**, *59*, 569−590.
(19) Azaïs, T.; Bonhomme, C.; Bonhomme-Coury, L.; Vaissermann, J.; Millot, Y.; Man, P. P.; Bertani, P.; Hirschinger, J.; Livage, J. *J. Chem. Soc., Dalton Trans.* **2002**, 609−618.
(20) Azaïs, T.; Bonhomme-Coury, L.; Vaissermann, J.; Bertani, P.; Hirschinger, J.; Maquet, J.; Bonhomme, C. *Inorg. Chem.* **2002**, *41*, 981−988.
(21) Franke, D.; Hudalla, R.; Maxwell, R.; Eckert, H. *J. Phys. Chem.* **1992**, *96*, 7506−7509.
(22) Lejeune, C.; Coelho, C.; Bonhomme-Coury, L.; Azaïs, T.; Maquet, J.; Bonhomme, C. *Solid State NMR* **2005**, *27*, 242−246.
(23) (a) King, I. J.; Fayon, F.; Massiot, D.; Harris, R. K.; Evans, J. S. O. *Chem. Commun.* **2001**, 1766−1767. (b) Fayon, F.; Massiot, D.; Suzuya, K.; Price, D. L. *J. Non-Cryst. Solids* **2001**, *283*, 88−94. (c) Fayon, F.; Le Saout, G.; Emsley, L.; Massiot, D. *Chem. Commun.* **2002**, 1702−1703. (d) Fayon, F.; King, I. J.; Harris, R. K.; Gover, R. K. B.; Evans, J. S. O.; Massiot, D. *Chem. Mater.* **2003**, *15*, 2234−2239. (e) Fayon, F.; King, I. J.; Harris, R. K.; Evans, J. S. O.; Massiot, D. *C. R. Chim.* **2004**, *7*, 351−361. (f) Feike, M.; Jäger, C.; Spiess, H. W. *J. Non-Cryst. Solids* **1998**, *223*, 200−206.
(24) (a) Hartmann, P.; Jana, C.; Vogel, J.; Jäger, C. *Chem. Phys. Lett.* **1996**, *258*, 107−112. (b) Clayden, N. J.; Esposito, S.; Aronne, A. J. *Chem. Soc., Dalton Trans.* **2001**, 2003−2008.
(25) (a) Fyfe, C. A.; Feng, Y.; Gies, H.; Grondey, H.; Kokotailo, G. T. *J. Am. Chem. Soc.* **1990**, *112*, 3264−3270. (b) Fyfe, C. A.; Wong-Moon, K. C.; Huang, Y.; Grondey, H. *J. Am. Chem. Soc.* **1995**, *117*, 10397−10398. (c) Bechmann, M.; Helluy, X.; Marichal, C.; Sebald, A. *Solid State NMR* **2002**, *21*, 71−85.
(26) Franke, D.; Hudalla, C.; Eckert, H. *Solid State NMR* **1992**, *1*, 33−40.
(27) (a) Lesage, A.; Auger, C.; Caldarelli, S.; Emsley, L. *J. Am. Chem. Soc.* **1997**, *119*, 7867−7868. (b) Lesage, A.; Bardet, M.; Emsley, L. *J. Am. Chem. Soc.* **1999**, *121*, 10987−10993. (c) Sakellariou, D.; Brown, S. P.; Lesage, A.; Hediger, S.; Bardet, M.; Meriles, C.; Pines, A.; Emsley, L. *J. Am. Chem. Soc.* **2003**, *125*, 4376−4380.
(28) (a) Lesage, A.; Sakellariou, D.; Steuernagel, S.; Emsley, L. *J. Am. Chem. Soc.* **1998**, *120*, 13194−13201. (b) Lesage, A.; Charmont, P.; Steuernagel, S.; Emsley, L. *J. Am. Chem. Soc.* **2000**, *122*, 9739−9744.
(29) Fayon, F.; Massiot, D.; Levitt, M. H.; Titman, J. J.; Gregory, D. H.; Duma, L.; Emsley, L.; Brown, S. P. *J. Chem. Phys.* **2005**, *122*, 194313.
(30) (a) Hedin, N.; Graf, R.; Christiansen, S. C.; Gervais, C.; Hayward, R. C.; Eckert, J.; Chmelka, B. F. *J. Am. Chem. Soc.* **2004**, *126*, 9425−9432. (b) Brouwer, D. H.; Kristiansen, P. E.; Fyfe, C. A.; Levitt, M. H. *J. Am. Chem. Soc.* **2005**, *127*, 542−543.
(31) (a) Brown, S. P.; Pérez-Torralba, M.; Sanz, D.; Claramunt, R. M.; Emsley, L. *J. Am. Chem. Soc.* **2002**, *124*, 1152−1153.(b) Brown, S. P.; Pérez-Torralba, M.; Sanz, D.; Claramunt, R. M.; Emsley, L. *Chem. Commun.* **2002**, *17*, 1852−1853.
(32) (a) Grasso, G.; De Swiet, T. M.; Titman, J. J. *J. Phys. Chem. B* **2002**, *106*, 8676−8680. (b) Olsen, R. A.; Struppe, J.; Elliott, D. W.; Thomas, R. J.; Mueller, L. J. *J. Am. Chem. Soc.* **2003**, *125*, 11784−11785. (c) De Paëpe, G.; Lesage, A.; Steuernagel, S.; Emsley, L. *Chem. Phys. Chem.* **2004**, *5*, 869−875. (d) Cadars, S.; Lesage, A.; Emsley, L. *J. Am. Chem. Soc.* **2005**, *127*, 4466−4476. (e) Harris, R. K.; Joyce, S. A.; Pickard, C. J.; Emsley, L. *Phys. Chem. Chem. Phys.* **2006**, *8*, 137−143.
(33) Massiot, D.; Fayon, F.; Alonso, B.; Trebosc, J.; Amoureux, J. P. *J. Magn. Reson.* **2003**, *164*, 160−164.
(34) Iuga, D.; Morais, C.; Gan, Z.; Neuville, D. R.; Cormier, L.; Massiot, D. *J. Am. Chem. Soc.* **2005**, *127*, 11540−11541.
(35) Coelho, C.; Azaïs, T.; Bonhomme-Coury, L.; Maquet, J.; Massiot, D.; Bonhomme, C. *J. Magn. Reson.* **2006**, *179*, 114−119.
(36) Montouillout, V.; Morais, C. M.; Douy, A.; Fayon, F.; Massiot, D. *Magn. Reson. Chem.* **2006**, *44*, 770−775.
(37) Fayon, F.; Roiland, C.; Emsley, L.; Massiot, D. *J. Magn. Reson.* **2006**, *179*, 49−57.
(38) (a) Deschamps, M.; Fayon, F.; Montouillout, V.; Massiot, D. *Chem. Commun.* **2006**, 1924−1925. (b) Deschamps, M.; Massiot, D. *J. Magn. Reson.* **2006**, published online.

pulse schemes.[39] Solid-state COSY (correlation spectroscopy),[25a,c] TOBSY (total through-bond correlation spectroscopy),[40] and *J*-resolved experiments[23d−e,33,41] were also used for the characterization of organic and inorganic derivatives.

The INEPT (insensitive nuclei enhanced by polarization transfer) sequence[42] is a routine pulse block for a large variety of solution-state multidimensional experiments.[43] The main advantage of this sequence is the efficient through-bond transfer of polarization from an abundant spin system (such as ^{1}H or ^{31}P) to a low-abundance spin system (such as ^{13}C or ^{29}Si). In the frame of solid-state NMR, the INEPT sequence was adapted for the study of mobile[44] and rigid[45] organic and hydrid systems. When dealing with inorganic derivatives, very few examples were published in the literature, involving mainly the $^{27}Al/^{31}P$ spin pair,[25b,46−49] and two specific minerals, namely, the microcline ($^{27}Al/^{29}Si$) and the albite ($^{23}Na/^{29}Si$).[25b] The recent interest in *J*-MAS derived NMR techniques is essentially due to the fact that the involved coherence lifetimes are long enough for efficient polarization transfer and that the refocused line widths are much smaller than the apparent line widths, as discussed recently in the literature.[32c,50]

In this paper, we show that the $^{31}P-^{29}Si$ MAS-*J*-INEPT experiment can act as an invaluable tool of investigation for silicophosphate derivatives. Efficient through-bond polarization transfer is first demonstrated for the crystalline $Si_5O(PO_4)_6$ phase.[51] The 1D MAS-*J*-INEPT build-up curves are analyzed in terms of SI_n ($n \leq 6$) or $SI_nI'_n$ ($n = 3$) spin systems ($S = ^{29}Si$, $I = ^{31}P$), leading to the determination of the $^{2}J_{P-O-Si}$ coupling constants. It is shown that the $^{2}J_{P-O-Si}$ coupling constants are strongly dependent on the crystallographic chemical paths. To the best of our knowledge, such constants have not been reported so far in the literature even in the frame of solution-state NMR. The extension of the MAS-*J*-INEPT approach to 2D experiments leads to the unambiguous description of crystalline silicophosphate mix-
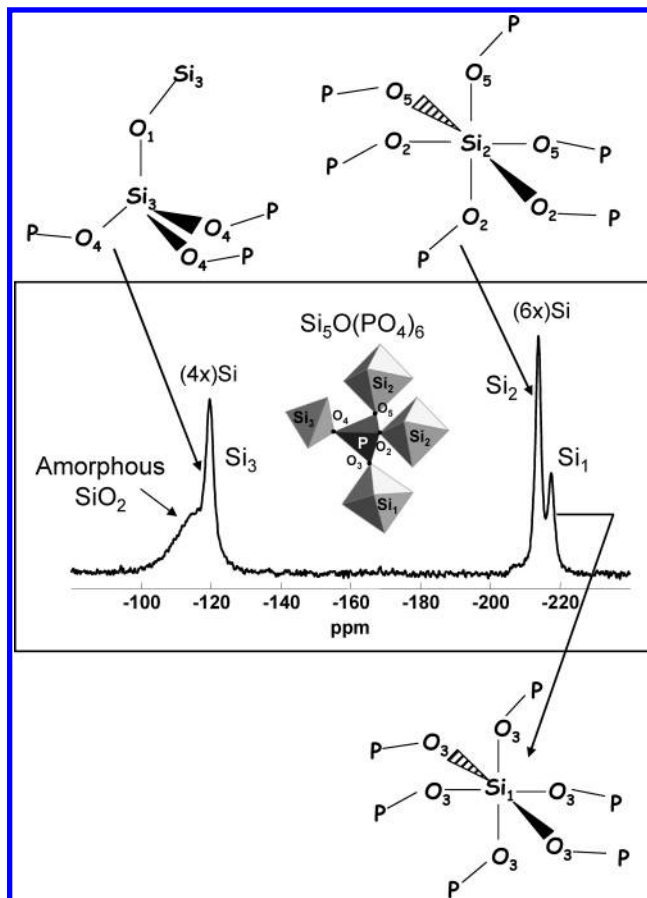

Figure 1. Description of the structure of $Si_5O(PO_4)_6$ around the P and Si atoms. The labelling scheme of atoms is given according to the literature.[51] ^{29}Si MAS spectrum (single-pulse experiment) (Ø, 4 mm; rotation frequency (RO), 14 kHz; number of scans (NS), 1760; recycle delay (RD), 10 s; 90°- (^{29}Si), 4.5 μs; LB = 10 Hz).

tures, involving SiP_2O_7 polymorphs.[24a,35,52] Finally, the MAS-*J*-INEPT experiment is also adapted for the study of amorphous silicophosphate gels,[1−3] revealing interesting structural features. The INEPT through-bond approach appears very robust and less demanding in terms of RF power levels, when compared to the $^{31}P \rightarrow ^{29}Si$ CP MAS experiment (indeed, short $\pi/2$ and π pulses are used in the INEPT sequence instead of long contact time pulses). We strongly believe that the MAS-*J*-INEPT technique is suitable for the fine characterization of the derivatives cited above in points i−iv.

Experimental Section

Solid-state NMR experiments were performed on a Bruker AVANCE 300 spectrometer at $B_0 = 7$ T with $\nu_0(^{31}P) = 121.49$ MHz and $\nu_0(^{29}Si) = 59.63$ MHz, using a 4 mm triple-resonance Bruker MAS probe. The spinning rate was 14 kHz, and samples were spun at the magic angle using ZrO_2 rotors. The setting of the magic angle was carefully checked. For the MAS-*J*-INEPT experiments in one and two dimensions, the τ and τ' delays were

(39) (a) Trebosc, J.; Amoureux, J. P.; Wiench, J. W.; Pruski, M. *Chem. Phys. Lett.* **2003**, *374*, 432−438. (b) Trebosc, J.; Amoureux, J. P.; Delevoye, L.; Wiench, J. W.; Pruski, M. *Solid State Sci.* **2004**, *6*, 1089−1095. (c) Amoureux, J. P; Trebosc, J.; Wiench, J.; Massiot, D.; W.; Pruski, M. *Solid State NMR* **2005**, *27*, 228−232.
(40) (a) Baldus, M.; Meier, B. H. *J. Magn. Reson. A* **1996**, *121*, 65−69. (b) Helluy, X.; Marichal, C.; Sebald, A. *J. Phys. Chem. B* **2000**, *104*, 2836−2845.
(41) Miura, H.; Terao, T.; Saika, A. *J. Magn. Reson.* **1986**, *68*, 593−596.
(42) (a) Morris, G. A.; Freeman, R. *J. Am. Chem. Soc.* **1979**, *101*, 760− 762. (b) Burum, D. P.; Ernst, R. R. *J. Magn. Reson.* **1980**, *39*, 163− 168. (c) Sorensen, O. W.; Ernst, R. R. *J. Magn. Reson.* **1983**, *51*, 477−489.
(43) (a) Levitt, M. H. *Spin Dynamics, Basics of Nuclear Magnetic Resonance*; Wiley: Chichester, U.K., 2002. (b) Keeler, J. *Understanding NMR Spectroscopy*; Wiley: Chichester, U.K., 2005.
(44) (a) Soubias, O.; Reat, V.; Saurel, O.; Milon, A. *J. Magn. Reson.* **2002**, *158*, 143−148. (b) Alonso, B.; Massiot, D. *J. Magn. Reson.* **2003**, *163*, 347−352.
(45) Elena, B.; Lesage, A.; Steuernagel, S.; Böckmann, A.; Emsley, L. *J. Am. Chem. Soc.* **2005**, *127*, 17296−17302.
(46) Kao, H. M.; Grey, C. P. *J. Magn. Reson.* **1998**, *133*, 313−323.
(47) Fyfe, C. A.; Meyer zu Altenschildesche, H.; Wong-Moon, K. C.; Grondey, H.; Chezeau, J. M. *Solid State NMR* **1997**, *9*, 97−106.
(48) Wiench, J. W.; Pruski, M. *Solid State NMR* **2004**, *26*, 51−55.
(49) Kao, H. M.; Grey, C. P. *J. Am. Chem. Soc.* **1997**, *119*, 627−628.
(50) Lesage, A.; Duma, L.; Sakellariou, D.; Emsley, L. *J. Am. Chem. Soc.* **2001**, *123*, 5747−5752.
(51) Mayer, H. *Monatsh. Chem.* **1974**, *105*, 46−53.

(52) (a) Krawietz, T. R.; Lin, P.; Lotterhos, K. E.; Torres, P. D.; Barich, D. H.; Clearfield, A.; Haw, J. F. *J. Am. Chem. Soc.* **1998**, *120*, 8502− 8511. (b) Poojary, D. M.; Borade, R. B.; Campbell, F. L.; Clearfield, A. *J. Solid State Chem.* **1994**, *112*, 106−112. (c) Mudrakovskii, I. L.; Mastikhin, V. M.; Shmachkova, V. P.; Kotsarenko, N. S. *Chem. Phys. Lett.* **1985**, *120*, 424−426.

Table 1. [31]P and [29]Si Isotropic Chemical Shifts for $Si_5O(PO_4)_6$ (Si_5P_6) and the Various SiP_2O_7 Polymorphs[a]

phase (JCPDS)	δ_{iso} (ppm) ^{31}P MAS	δ_{iso} (ppm) ^{31}P INEPT	δ_{iso} (ppm) [29]Si INEPT
$Si_5O(PO_4)_6$ (70-2071)	−43.8	−43.9	−119.3
			−213.5
			−217.3
SiP_2O_7 tetragonal (22-1320)	−45.5	−45.6	−213.0
	−52.8	−52.9	
SiP_2O_7 monoclinic 1 (39-0189)	−47.6	−47.7	−215.3
	−55.3	−55.4	
SiP_2O_7 monoclinic 2 (25-0755)	−46.1		
	−49.4		
SiP_2O_7 cubic (22-1321)	∼ −50		
	∼ −58		
	∼ −70		

[a] [31]P MAS, single-pulse experiments; ^{31}P/[29]Si INEPT, projections of the 2D [31]P−[29]Si MAS-*J*-INEPT experiments.
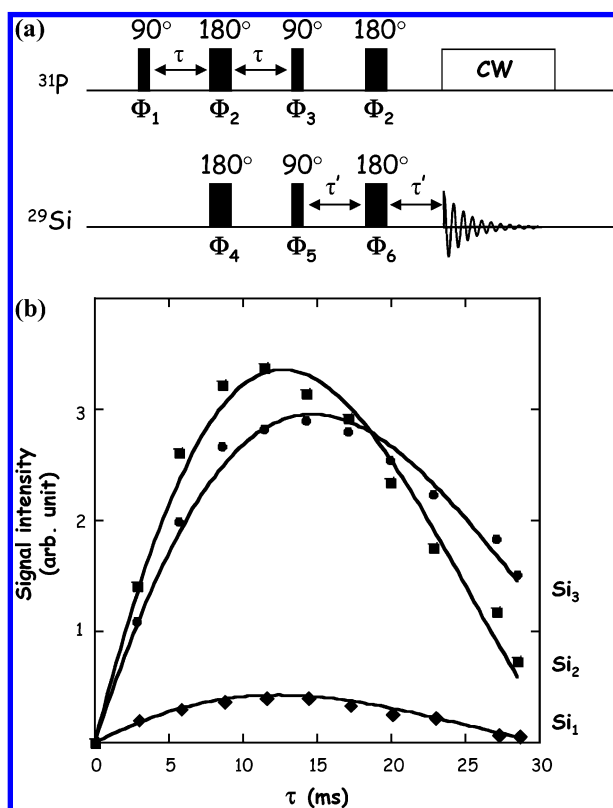

Figure 2. (a) 1D refocused [31]P−[29]Si MAS-*J*-INEPT pulse sequence. Phase cycling: Φ_1 = +x, +x, +x, +x, +x, +x, +x, +x, −x, −x, −x, −x, −x, −x, −x, −x; Φ_2 = +x, −x; Φ_3 = +y, +y, −y, −y; Φ_4 = +x, −x; Φ_5 = +x, +x, +x, +x, +y, +y, +y, +y, −x, −x, −x, −x, −y, −y, −y, −y; Φ_6 = +x, −x, +x, −x, +y, −y, +y, −y; receiver = +x, +x, −x, −x, +y, +y, −y, −y. (b) Experimental evolution of [29]Si MAS-*J*-INEPT intensities as a function of τ (with τ′ = 11 ms) for Si_1, Si_2, and Si_3 ($Si_5O(PO_4)_6$ phase).

synchronized with the rotor period. The INEPT build-up curves were established independently for the 4- and 6-fold coordinated [29]Si sites, by varying the [29]Si offset (to minimize off-resonance effects) (see below). The same experimental approach was applied for the measurement of T_2' constants by MAS spin−echo experiments. [31]P chemical shifts were referenced to 85% aqueous H_3PO_4. [29]Si chemical shifts were referenced to TMS. Full experimental details are given in the figure captions.

The synthesis protocols of the $Si_5O(PO_4)_6$ phase and of the various polymorphs of SiP_2O_7 are the following. For *crystalline*

Table 2. Estimated T_2'([29]Si) and T_2'(^{31}P) Obtained using MAS Spin−Echo Experiments and eq 1 for the $Si_5O(PO_4)_6$ (Si_5P_6) Phase (Si_1, Si_2, Si_3, and P sites)

	T_2'([29]Si) (ms)	T_2'(^{31}P) (ms) [35]
Si_1−O−P	41 ± 4	65 ± 3
Si_2−O−P	55 ± 4	
Si_3−O−P	63 ± 5	

$Si_5O(PO_4)_6$, TEOS ($Si(OCH_2CH_3)_4$) (44.80 mmol, 5.16 g), ethanol, and distilled water were used as precursors (TEOS/EtOH/H_2O = 1:4:3). The phosphorus precursor H_3PO_4 (85%) was added (44.8 mmol, 5.16 g) at room temperature. The reaction was slightly exothermic. The doping by a paramagnetic complex $NiCl_2$·$6H_2O$ (1% molar ratio) was performed for relaxation purposes (see below), leading to a slightly green solution. After the mixture was stirred at 25 °C, a transparent green wet gel was obtained (2 h). The final powder was obtained after heat treatment at 800 °C for 2 h. For the *mixture of the SiP_2O_7 polymorphs and $Si_5O(PO_4)_6$*, after the dissolution of 0.05 g (0.22 mmol) of $NiCl_2$·$6H_2O$ in ethanol, 5.16 g (44.80 mmol) of H_3PO_4 were added, followed by 4.67 g (22.40 mmol) of TEOS. A gel was obtained after 2 h at room temperature, then heated at 100 °C for 48 h, and subsequently, heated at 1000 °C for 2 h. The *SiP-136 silicophosphate gel* was prepared by the sol−gel process using TEOS ($Si(OCH_2CH_3)_4$, ethanol, and distilled water as precursors (TEOS/EtOH/H_2O = 1:4:3). At room temperature, the phosphorus precursor (H_3PO_4 85% phosphoric acid) was added (Si/P = 1:1).[2] The doping by Ni^{2+} was performed as well, leading to a slightly green solution. A transparent green wet gel was obtained (2 h). A powder was obtained after 6 days at 136 °C. The temperature has a major impact on the involved species. The choice of 136 °C is related to the presence of both amorphous and crystalline components. Moreover, the obtained gels are highly sensitive to air moisture, leading to completely different spectroscopic characteristics upon aging. The gel was therefore carefully kept under a dry atmosphere and subsequently analyzed.

The addition of $NiCl_2$·$6H_2O$ led to a drastic reduction of T_1(^{31}P) (∼1 s). Indeed, T_1(^{31}P) have been estimated to ∼40 s for gels and ∼480 s for crystalline silicophosphate phases.[22] The percent molar ratio of paramagnetic complex was adjusted to obtain shortened T_1(^{31}P) and T_1([29]Si), without drastic modification of the line widths and of the characteristic T_2' of the various resonances. The notion of T_2' constant is essential for the evolution of the coherences involved in the *J*-derived experiments and will be explained below.

Results and Discussion

$Si_5O(PO_4)_6$ Crystalline Phase. The structure of $Si_5O(PO_4)_6$ described by Mayer[51] (trigonal, $R\bar{3}$, a = 7.869 Å, c = 24.138 Å) involves one unique P site and three inequivalent Si sites (two 6-fold coordinated Si_{VI} atoms, Si_1 and Si_2, and one 4-fold coordinated, Si_{IV} atom Si_3). The Si_1/Si_2/Si_3 ratio is 1:2:2. The structure consists of [SiO_6] and [Si_2O_7] groups linked by [PO_4] groups. Each [PO_4] tetrahedron is surrounded by three Si_{VI} atoms (Si_2 (×2) and Si_1) and one Si_{IV} atom (Si_3) (Figure 1). The Si_1 atom is bonded to six equivalent oxygen atoms O_3 (Si_1O_3= 1.756 Å, Si_1O_3P = 145.58°). Consequently, the six involved P−O_3−Si_1 bonds are equivalent. The Si_2 atom is bonded to six oxygen atoms, but two inequivalent oxygen atoms (O_2 and O_5) are involved (Si_2O_2 = 1.791 Å, Si_2O_5 = 1.756 Å, Si_2O_2P = 131.15°, Si_2O_5P= 151.38°). The three P−O_4−Si_3 bonds involved in
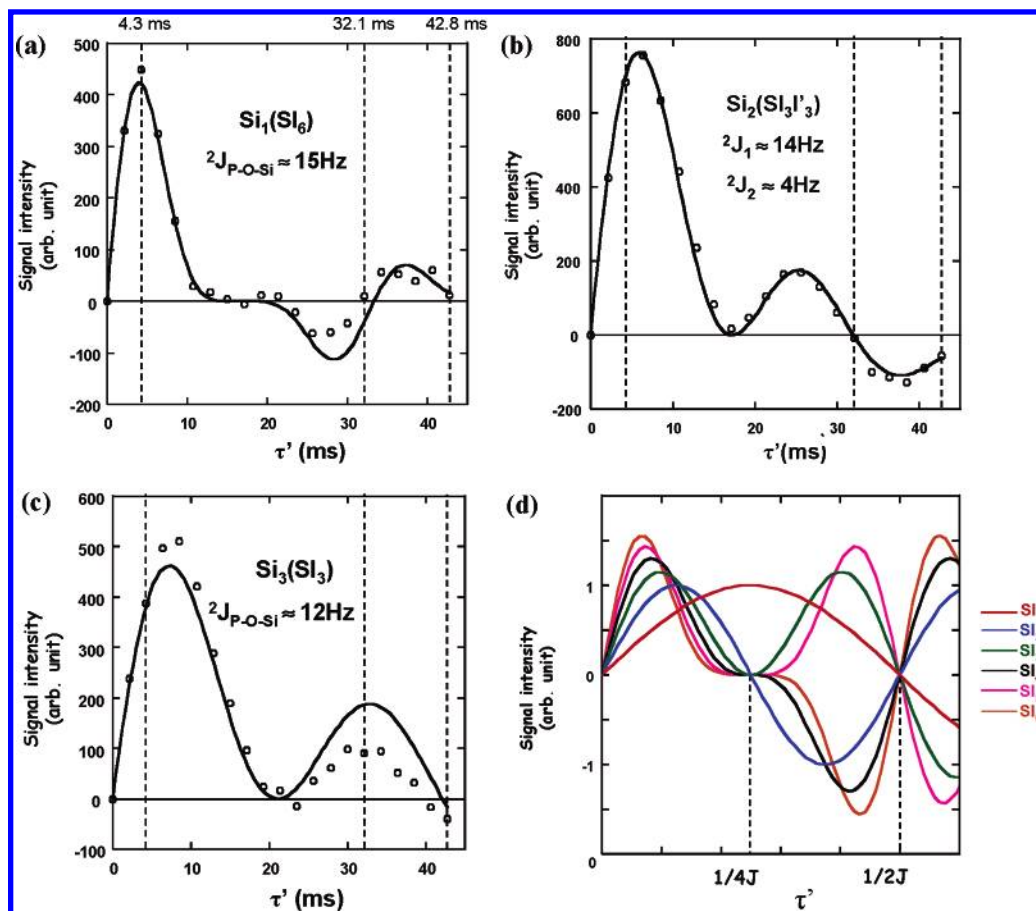
Figure 3. (a−c). Experimental evolution of ^{29}Si MAS-*J*-INEPT intensities as a function of τ' (with $\tau = 11.4$ ms) for Si_1, Si_2, and Si_3 ($Si_5O(PO_4)_6$ phase), respectively. The experimental data (○) were fitted by the eqs 2 for Si_1 and Si_3 and 4 for Si_2. The fixed T_2' constants are extracted from spin echo experiments (Table 2) (Ø, 4 mm; RO, 14 kHz; NS, 656; RD, 5 s; 90°(^{29}Si), 5.3 μs; 90°(^{31}P), 5 μs). (d) Theoretical curves (versus τ', at fixed τ delay) for the SI_n spin systems ($1 \le n \le 6$), following eq 2 with one unique *J* coupling constant and neglecting all T_2' effects.

the Si_3 tetrahedron are equivalent ($Si_3O_4 = 1.611$ Å, $Si_3O_4P = 138.83°$). The fourth Si_3-O bond is connected to a Si_{IV} tetrahedron.

The ^{31}P MAS spectrum reveals a unique resonance located at $\delta(^{31}P) = -43.8$ ppm, while the ^{29}Si MAS spectrum exhibits three resonances located at $\delta(^{29}Si) = -119.3$, -213.5, and -217.3 ppm (Figure 1 and Table 1). A broad resonance centered at $\delta(^{29}Si) \approx -113.5$ ppm associated with amorphous silica SiO_2 (side product) is also evidenced.

The pulse sequence for the solid-state refocused $^{31}P-^{29}Si$ MAS-*J*-INEPT experiment is shown in Figure 2a. The original solution-state technique[42] was adapted here for rotating solids and for a new pair of nuclei $^{31}P-^{29}Si$. Fast magic angle spinning (usually 14 kHz) averages the chemical shift anisotropy and the heteronuclear dipolar couplings to zero, leaving only the scalar couplings and the isotropic chemical shifts.[45] The refocused INEPT pulse sequence consists of the following steps: a 90° pulse is applied to the ^{31}P channel, followed by an evolution delay optimized to achieve ^{31}P antiphase magnetization. The refocusing of the isotropic chemical shifts is obtained by the simultaneous application of 180° pulses on both phosphorus-31 and silicon-29 channels (only the $^2J_{P-O-Si}$ couplings have to be taken into account). For a pair of ^{31}P and ^{29}Si nuclei involved in a $^{31}P-O-^{29}Si$ group, antiphase phosphorus-31 coherence with

respect to silicon-29 is created after the first $\tau-\pi-\tau$ period. The two simultaneous 90° pulses lead to antiphase silicon-29 coherence. The refocusing period $\tau'-\pi-\tau'$ is then applied to obtain in-phase ^{29}Si magnetization. Note that ^{31}P decoupling is applied during the acquisition of the ^{29}Si signal.

In the MAS-*J*-INEPT experiment, the two τ and τ' delays must be carefully optimized. Such parameters involve not only the value of the $^2J_{P-O-Si}$ coupling constants but also the relaxation time T_2' associated to each site. The T_2' time constant corresponds to the non-refocusable line width (namely $\Delta' = 1/\pi T_2'$) which is usually significantly narrower than the "apparent" line width. Following the discussion of Emsley and co-workers,[27−28,32c−e,50] we use the notation T_2' which clearly states the experimental nature of this relaxation time and makes no hypothesis on its underlying mechanism.[33] It is possible to estimate the T_2' parameter by using a simple MAS spin−echo experiment 90°−τ−180°−τ. The corresponding decay curves versus 2τ (not presented here) were fitted in the time domain by a single-exponential time constant, according to

$$I_{echo} = \exp{(-2\tau/T_2')} \qquad (1)$$

leading therefore to an estimate of T_2' for the ^{29}Si and ^{31}P resonances (see Table 2). For the refocused INEPT
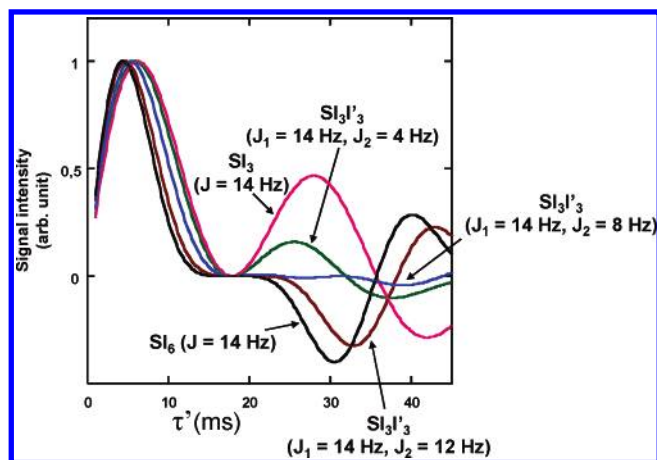
Figure 4. Theoretical curves (versus τ', at fixed τ delay) for SI_3, SI_6, and $SI_3I'_3$ spin systems following eq 4 with various (J_1, J_2) coupling constants. $T_2'(^{29}Si)$ for Si_2 is extracted from spin echo experiments (Table 2).

experiment and considering a *unique* $^2J_{P-O-Si}$ coupling constant, the signal intensity is proportional to the product[43,53−54]

$$I_{INEPT}(\tau,\tau') = I_0 \sin(2\pi\,^2J_{P-O-Si}\tau)$$
$$\sin(2\pi\,^2J_{P-O-Si}\tau') \cos^{(n-1)}(2\pi\,^2J_{P-O-Si}\tau')$$
$$\times \exp(-2\tau/T_2'(^{31}P)) \exp(-2\tau'/T_2'(^{29}Si)) \quad (2)$$

where n is the bond multiplicity (i.e., SI_n spin system with $S \equiv\ ^{29}Si$ and $I \equiv\ ^{31}P$). Neglecting all T_2' effects, the ^{29}Si signal is maximized by choosing $\tau = 1/4J_{^{31}P-O-^{29}Si}$. Figure 2b presents the experimental ^{29}Si signal intensities obtained by varying τ (τ' being fixed to 11 ms) for Si_1, Si_2, and Si_3. An optimum located at $\tau = 11.4$ ms is observed and will be used as a constant thereafter. As in solution state NMR, the MAS-*J*-INEPT experiment can be safely implemented for editing purposes. The build-up curves obtained versus τ' (at fixed $\tau = 11.4$ ms) for Si_1, Si_2, and Si_3 are presented in Figure 3a−c. The variation of the intensities is clearly distinct, depending on both the number of $(-OP)$ bonds around the silicon atoms ($n = 6$ for Si_1, Si_2; $n = 3$ for Si_3) and the crystallographic characteristics of the various sites (for Si_1 and Si_2). To the best of our knowledge, we present here for the first time the build-up curves related to SI_n spin systems with $n > 3$ (in the solid state). Examples dealing with $n < 4$ are related mainly to CH_n groups in *solution-state* NMR. Editing is achieved. (i) For $\tau' = 4.3$ ms, all resonances are positive. (ii) For $\tau' = 32.1$ ms, the (Si_1, Si_2) resonances are almost zero, and the Si_3 resonance is positive. (iii) For $\tau' = 42.8$ ms, all resonances are negative or almost zero. The theoretical curves corresponding to $n = 1, 2, ..., 6$ (SI_n spin systems) are presented in Figure 3d (neglecting all T_2' relaxation effects). A unique J coupling constant is considered. The maximum transfer ranges from 1 (in arbitrary units) for a SI spin system to 1.55 for a SI_6 spin system.[53] Moreover,

(53) Pegg, D. T.; Doddrell, D. M.; Brooks, W. M.; Bendall, M. R. *J. Magn. Reson.* **1981**, *44*, 32−40.
(54) Lux, P.; Brunet, F.; Desvaux, H.; Virlet, J. *Magn. Reson. Chem.* **1993**, *31*, 623−631.

τ'_{max} is given by[53]

$$\tau'_{max} = 1/2\pi J \arcsin[n^{-1/2}] \quad (3)$$

The intensity evolution is governed by the product of two terms, namely, $\cos^{(n-1)}(2\pi\,^2J_{P-O-Si}\tau')$ (0 for $\tau' = 1/4J$) and $\sin(2\pi\,^2J_{P-O-Si}\tau')$ (0 for $\tau' = 1/2J$). For $n = 1$, a simple sine evolution is observed. An important parameter is the *parity* of the multiplicity n. Indeed, for *odd n* values, the signal intensity is always positive for τ' varying between 0 and $1/2J$. For *even n* values, the signal intensity is positive for $\tau' = 0 \rightarrow 1/4J$ and then negative for $\tau' = 1/4J \rightarrow 1/2J$. For increasing *even n* values, a flat evolution of the intensity is observed around $\tau' \approx 1/4J$. The eq 2, as well as the T_2' constants presented in Table 2, were used for the fitting of the experimental curves for Si_1 and Si_3. For both ^{29}Si sites, a unique $^2J_{P-O-Si}$ coupling constant is involved (see Figure 1). The Si_1 build-up curve (Figure 3a) is characteristic for an even n value (positive and negative intensity) with a flat evolution around $\tau' \approx 16$ ms (i.e., $n = 6$). The extracted J value corresponds to $^2J_{P-O-Si} \approx 15$ Hz. The Si_3 build-up curve (Figure 3c) is characteristic of an odd n value (i.e., $n = 3$). The extracted J value corresponds to $^2J_{P-O-Si} \approx 12$ Hz. Obviously, the Si_2 build-up curve differs drastically from the one obtained for Si_1, even though Si_1 and Si_2 correspond both to 6-fold coordinated silicon atoms. In the case of Si_2, two different $^2J_{P-O-Si}$ coupling constants have to be a priori considered corresponding to Si_2-O_2-P and Si_2-O_5-P bonding paths (see Figure 1). With two distinct J coupling constants (J_1 and J_2, $SI_3I'_3$ spin system), the product operator formalism,[43] leads to the MAS-*J*-INEPT intensity given by

$$I_{INEPT}(\tau,\tau') = I_0 \cos^2(2\pi J_1\tau') \cos^2(2\pi J_2\tau') [\sin(2\pi J_1\tau)$$
$$\sin(2\pi J_1\tau') \cos(2\pi J_2\tau') + \sin(2\pi J_2\tau) \sin(2\pi J_2\tau')$$
$$\cos(2\pi J_1\tau')] \times \exp(-2\tau/T_2'(^{31}P)) \exp(-2\tau'/T_2'(^{29}Si)) \quad (4)$$

For $J_1 = J_2$, eq 4 is comparable to eq 2 with $n = 6$. For $J_2 = 0$ Hz, eq 4 is comparable to eq 2 with $n = 3$. By considering the Figures 3a and 3b, we can exclude $J_1 \approx J_2$ because no flat evolution is observed for Si_2 as it would be for a SI_6 case. Various theoretical curves using eq 4 are presented in Figure 4 for various (J_1, J_2) values. The curves corresponding to $J_1 = J_2$ and $n = 3, 6$ (SI_3 and SI_6 spin systems) are also presented. At a fixed J_1 value (here $J_1 = 14$ Hz), strong differences in the build-up curves are observed for J_2 varying from 14 to 0 Hz. In particular, the MAS-*J*-INEPT intensity remains strictly positive for $\tau' \le 30$ ms and for $J_2 < 8$ Hz. The fitting of the Si_2 curve (Figure 3b) leads to $J_1 \approx 14$ Hz and $J_2 \approx 4$ Hz. The obtained J_2 value appears small, but several authors previously mentioned differences in J coupling constants, corresponding to different crystallographic paths.[33] We note that two distinct bond angles are involved in the case of Si_2 ($Si_2-O_2-P \approx 131°$ and $Si_2-O_5-P \approx 151°$) and could explain the strong difference between J_1 and J_2. The errors on the extracted J-coupling constants can be estimated to ± 2 Hz.

We have shown that the MAS-*J*-INEPT experiment was suitable for the fine description of $Si-O-P$ bonding in terms
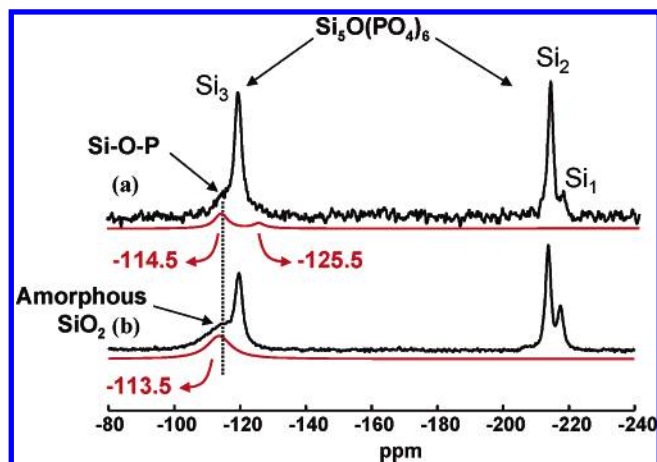
Figure 5. (a) 1D refocused $^{31}P-^{29}Si$ MAS-*J*-INEPT spectrum of $Si_5O(PO_4)_6$ (Ø, 4 mm; RO, 14 kHz; NS, 1440; RD, 5 s; 90°(^{29}Si), 5.3 μs; 90°(^{31}P), 5 μs; τ = 16.6 ms; τ'= 11.1 ms; LB = 10 Hz). The red lines correspond to the simulation of the broad components. (b) ^{29}Si MAS spectrum (single-pulse experiment) of $Si_5O(PO_4)_6$ (Ø, 4 mm; RO, 14 kHz; NS, 1760; RD, 10 s; 90°(^{29}Si), 4.5 μs; LB = 10 Hz).

of *J* coupling constants. The versatility of the experiment is further demonstrated by the fine-tuning of the (τ, τ') parameters, to reveal interesting chemical details. In that perspective, the Figure 5 shows the MAS-*J*-INEPT spectrum of $Si_5O(PO_4)_6$ for τ = 16.6 ms and τ' = 11.1 ms, as well as the corresponding ^{29}Si MAS spectrum (single pulse experiment). In the ^{29}Si MAS spectrum, a broad component located at $\delta \approx -113.5$ ppm is observed and primarily assigned to amorphous SiO_2. However, the $^{31}P-^{29}Si$ MAS-*J*-INEPT spectrum exhibits at least two broad slightly shielded components (centered at $\delta \approx -114.5$ ppm and $\delta \approx -125.5$ ppm, respectively, the latter being hardly discernible). These shielded components could be assigned to Q_4(^{29}Si) units involving at least one $^{29}Si-O-^{31}P$ group.[1d,3]

SiP_2O_7 Polymorphs and 2D MAS-*J*-INEPT Experiment. The extension of the MAS-*J*-INEPT experiment to the 2D spectra is now presented in the frame of the SiP_2O_7 polymorphs. The synthesis of SiP_2O_7 phases (see the Experimental Section) leads generally to mixtures of polymorphs and to complex ^{31}P MAS NMR spectra.[24a,35,52] We show that the 2D $^{31}P-^{29}Si$ MAS-*J*-INEPT experiment (Figure 6a) is suitable for the characterization of the various phases involved. The X-ray diffraction (XRD) powder pattern of the sample (not shown here) indicates that, in addition to the $Si_5O(PO_4)_6$ crystalline phase presented above, three polymorphs of SiP_2O_7 were synthesized as major constituents, namely, a tetragonal (JCPDS 22-1320) and two monoclinic forms (JCPDS 39-0189 monoclinic 1 and 25-0755 monoclinic 2). The cubic form of SiP_2O_7 (JCPDS 22-1321) is also present, as a very minor component. The various SiP_2O_7 phases involve pyrophosphate groups (Figure 6b). It is known from XRD data that the pyrophosphate groups (involving generally two nonequivalent P sites) are linked exclusively to Si_{VI} atoms. Figure 6c shows the ^{31}P MAS spectrum, exhibiting the tetragonal, monoclinic 1, monoclinic 2, and cubic forms of SiP_2O_7, as well as $Si_5O(PO_4)_6$. The assignments of the chemical shifts of the various phases were previously reported in the literature.[35] It shows also the
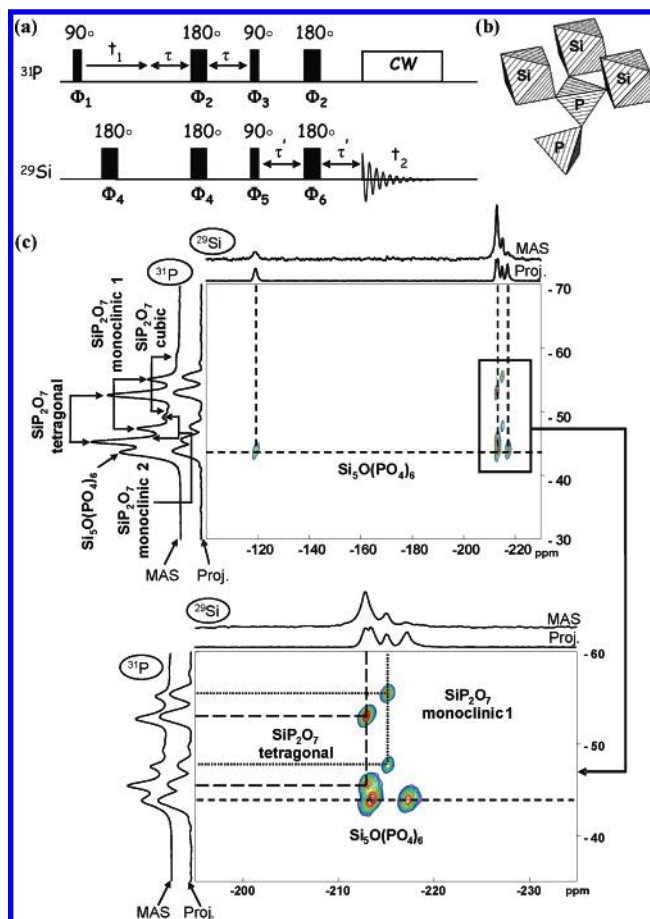

Figure 6. (a) 2D refocused $^{31}P-^{29}Si$ MAS-*J*-INEPT pulse sequence. (b) Structural scheme for SiP_2O_7 pyrophosphate groups: a given P atom is bonded to one P atom and three Si_{VI} atoms. (c) ^{31}P and ^{29}Si MAS spectra (single-pulse experiments) of the mixture of $Si_5O(PO_4)_6$ and SiP_2O_7 polymorphs (tetragonal, monoclinic 1, monoclinic 2, and cubic, see Table 1) (^{31}P Ø, 4 mm; RO, 14 kHz; NS, 8; recycle delay (RD), 5 s; 90°(^{31}P), 6 μs; LB = 0 Hz; ^{29}Si Ø, 4 mm; RO, 14 kHz; NS, 800; RD, 5 s; 90°(^{29}Si), 5.3 μs; LB = 20 Hz). The 2D refocused $^{31}P-^{29}Si$ MAS-*J*-INEPT spectrum of the mixture of $Si_5O(PO_4)_6$ and SiP_2O_7 polymorphs is also shown (Ø, 4 mm; RO, 14 kHz; NS, 496 for each t_1 increment; RD, 5 s; 90°(^{29}Si), 5.7 μs; 90°(^{31}P), 4.3 μs; τ = 11.4 ms; τ'= 4.6 ms; States mode with 128 t_1 increments, 88 h, LB = 20 Hz in $F($^{29}Si$)$, LB = 20 Hz in $F($^{31}P$)$. The expansion of the boxed region is presented in the bottom of the figure. The projections of the 2D spectrum are also given.

corresponding ^{29}Si MAS NMR spectrum. Resonances corresponding to 4- and 6-fold coordinated Si atoms are observed, with resolved components in the $-210/-220$ ppm region. The ^{31}P and ^{29}Si isotropic chemical shifts of the various SiP_2O_7 polymorphs are reported in Table 1.

Figure 6c shows also the 2D $^{31}P-^{29}Si$ MAS-*J*-INEPT spectrum of the $Si_5O(PO_4)_6$/SiP_2O_7 mixture (τ = 11.4 ms and τ' = 4.6 ms). Three cross-peaks associated to $Si_5O(PO_4)_6$ are observed (the ^{31}P resonance at -43.8 ppm correlates with three ^{29}Si resonances located at -119.3, -213.5, and -217.3 ppm). Moreover, the 2D spectrum reveals the presence of four other cross-peaks (shown in the expansion of the 2D spectrum). The ^{29}Si resonance at $\delta($^{29}Si$) = -213.0$ ppm correlates with two ^{31}P resonances located at -45.6 and -52.9 ppm, which are assigned to the tetragonal form of SiP_2O_7. The ^{29}Si resonance at $\delta($^{29}Si$) = -215.3$ ppm correlates with two ^{31}P resonances located at -47.7 and -55.4 ppm, which are assigned to the monoclinic 1 form of
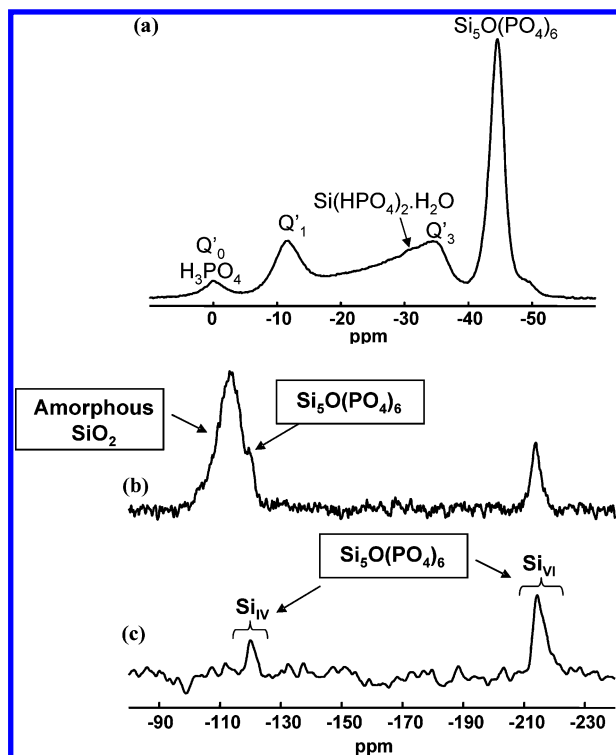
Figure 7. (a) ^{31}P MAS spectrum of the SiP-136 gel (Ø, 4 mm; RO, 14 kHz; NS, 16; RD, 5 s; 90°(^{31}P), 4.5 μs; LB = 20 Hz). (b) ^{29}Si MAS spectrum of the SiP-136 gel (Ø, 4 mm; RO, 14 kHz; NS, 1332; RD, 5 s; 90°(^{29}Si), 5.7 μs; LB = 20 Hz; ^{1}H decoupling). (c) 1D refocused ^{31}P–^{29}Si MAS-*J*-INEPT spectrum of the SiP-136 gel (Ø, 4 mm; RO, 14 kHz; NS, 2640; RD, 5 s; 90°(^{29}Si), 5.7 μs; 90°(^{31}P), 4.3 μs; τ = 11.4 ms; τ' = 4.6 ms; LB = 100 Hz).

SiP$_2$O$_7$ (Table 2). The ^{29}Si isotropic shift corresponding to each SiP$_2$O$_7$ polymorph is determined with great accuracy. The absence of observable cross-peaks for the monoclinic 2 and the cubic forms is surely related to the low amount of these particular phases or to the much lower $^2J_{P-O-Si}$ coupling constants and shorter T_2' constants. Such conclusions were also derived in the case of the MAS-*J*-HMQC experiment.[35] The HMQC and INEPT sequences are comparable when the experimental time is considered. However, the INEPT approach allows the clear distinction of the various Si resonances in terms of *J* coupling constants.

SiP-136 **Silicophosphate Gel.** Finally, the efficiency of the ^{31}P–^{29}Si MAS-*J*-INEPT technique is demonstrated for the study of complex systems, such as silicophosphate gels. The ^{31}P MAS spectrum of the SiP-136 gel is shown in Figure 7a. Broad resonances are observed and correspond to Q$'_N$ units (Q$'_N$ stands for P(O)(OY)$_N$(OY')$_{3-N}$ entities, with Y = P, Si ; Y' = H).[1d,3] In addition to a resonance at ~0 ppm corresponding to H$_3$PO$_4$ (Q$'_0$), three complex resonances are located at $\delta \approx$ −11, −35, and −44 ppm. Shoulders and minor components are also found. All these resonances can be assigned to Q$'_N$ species with *N* ranging from 0 to 3. The resonance at −11 ppm can be assigned to the Q$'_1$ units, but the chemical nature of the involved species is unfortunately not clearly defined (the notation Q$'_1$ implies one P−O−P bond and several P−(OX) bonds). The resonance at −44 ppm can be safely assigned to the crystalline Si$_5$O(PO$_4$)$_6$ phase described above. Moreover, the resonance centered

at δ = −30.8 ppm (hardly discernible because of the superimposition with a very broad component) can be assigned to Si(HPO$_4$)$_2$·H$_2$O.[52a] Both phases were clearly identified by powder XRD (not shown here) (Si$_5$O(PO$_4$)$_6$, JCPDS 70-2071; Si(HPO$_4$)$_2$·H$_2$O, JCPDS 18-1168). The protonation of the phosphate groups in the Si(HPO$_4$)$_2$·H$_2$O phase has been unambiguously proved by ^{1}H → ^{31}P CP MAS experiments reported in recent papers.[2−3] The ^{29}Si MAS spectrum of the SiP-136 gel is presented in Figure 7b. A rather broad peak at $\delta \approx$ −212 ppm is observed and corresponds to 6-fold coordinated Si atoms. This peak includes the resonances corresponding to the Si$_5$O(PO$_4$)$_6$ and Si(HPO$_4$)$_2$·H$_2$O phases. Moreover, a rather sharp line centered at $\delta \approx$ −119 ppm is superimposed to a much broader line (centered at $\delta \approx$ −114 ppm). This sharp line is safely assigned to the pyrosilicate species involved in the Si$_5$O(PO$_4$)$_6$ structure (Figure 1). We assume that the broad component corresponds to highly condensed Q$_4$ species with a certain amount of ^{29}Si−O−^{31}P groups. Figure 7c shows the 1D ^{31}P−^{29}Si MAS-*J*-INEPT spectrum of the SiP-136 gel (τ = 11.4 ms and τ' = 4.6 ms). The obtained spectrum exhibits two major resonances as expected, which are assigned to 4- and 6-fold coordinated Si atoms (corresponding to Si$_5$O(PO$_4$)$_6$ and Si(HPO$_4$)$_2$·H$_2$O). The broad component centered at $\delta \approx$ −114 ppm is efficiently suppressed, demonstrating again the efficiency of the INEPT sequence in terms of editing. Si−O−P linkages are not clearly seen (though the signal-to-noise ratio may not be sufficient). For this particular spectrum, the experimental time was 4 h, precluding therefore the use of the 2D MAS-*J*-INEPT correlation sequence. In a near future, efficient ^{1}H decoupling under fast MAS will be implemented to drastically increase the lifetime of the coherences involved in the MAS-*J*-INEPT sequence.[27−28,32c−e,50] 2D spectra should then be obtained in a reasonable time.

Conclusion

We have shown that the extension of the original refocused INEPT pulse scheme to the ^{31}P−^{29}Si MAS-*J*-INEPT experiment is suitable for the description of silicophosphate derivatives (crystalline phases and amorphous gels). Complex spin systems, involving up to *seven* spins, were taken into account for the detailed analysis of the INEPT build-up curves. $^2J_{P-O-Si}$ coupling constants were shown to depend on both the number of (−OP) bonds around the Si atoms and the various crystallographic paths involved. At this stage, *first principles* calculations of such coupling constants would be of crucial interest for the fine description of the P−O−Si bonds.[55] Moreover, such calculations could be validated by *J*-derived techniques, such as the MAS-*J*-INEPT experiment described above. From a fundamental point of view, the Si$_5$P$_6$ phase and the SiP$_2$O$_7$ polymorphs are characterized by very interesting SI$_n$ spin systems with $n \leq 6$. This particular situation is rarely encountered, and such spin

(55) (a) Pickard, C. J.; Mauri, F. *Phys. Rev. B* **2001**, 63, 245101-1-13. (b) Gervais, C.; Dupree, R.; Pike, K.; Bonhomme, C.; Profeta, M.; Pickard, C. J.; Mauri, F. *J. Phys. Chem. A* **2005**, 109, 6960−6969.

systems could be used as experimental standards for the set up of "optimized sequences".[56] Indeed, such sequence are designed for achieving the *maximum* transfer of polarization between the S spin (here, ^{29}Si) and the *n* spins I (here, ^{31}P).

The versatility of the MAS-*J*-INEPT approach in 1D and 2D versions has been demonstrated for the study of complex mixtures of crystalline phases and ill-crystallized gels obtained by sol−gel routes. Work is in progress in the laboratory for the extension of the $^{31}P-^{29}Si$ INEPT approach to the study of biomaterials involving silica and phosphate groups.

IC061964F

(56) Glaser, S. J.; Schulte-Herbrüggen, T.; Sieveking, M.; Schedletzky, O.; Nielsen, N. C.; Sorensen, O. W.; Griesinger, C. *Science* **1998**, *208*, 421−424.